

Hybrid Antenna-Amplifier: a Concept of High-Power Microwave Source and First Results of Its Exploration¹

A.S. Shlapakovski, I.I. Vintizenko, A.V. Petrov, E. Schamiloglu*

Nuclear Physics Institute at Tomsk Polytechnic University, 2a Lenina Str., Tomsk, 634050, Russia

Phone: 7-382-241-7959; Fax: 7-382-242-3934; E-mail: shl@npi.tpu.ru

** University of New Mexico, Albuquerque NM, 87131, USA*

Abstract – The concept of a hybrid antenna-amplifier device, that is a combination of a surface wave antenna with a relativistic Cherenkov amplifier, is set out. The key feature of the device providing its potential for a compact controllable high-power microwave source is that a rod antenna feed waveguide serves, at the same time, as a hollow cathode holder of a diode producing a relativistic electron beam. This is possible if a beam is generated using a compact module of a linear induction accelerator (LIA). The results obtained in the scope of exploration of this concept are reported. This includes the linear theory, 1-D nonlinear multi-mode theory, design of the LIA module, initial results of the 3-D simulations using the MAGIC code, and first results of model experiments on annular beam transport with a rod antenna inside.

1. Introduction

If a relativistic electron beam drifts along a surface wave antenna, it can amplify an antenna feed microwave signal due to Cherenkov interaction mechanism. Thus, a hybrid device is possible, which was called an antenna-amplifier [1, 2]. The concept of a hybrid antenna-amplifier embodies the idea that a compact high-power microwave source might be obtained through the integration of the electron beam accelerator and electrodynamic interaction space with a radiating antenna [3]. In this configuration, there is neither need for a microwave transmission line between the amplifier and antenna, nor for a mode converter providing appropriate field structure to antenna feeding. The benefit added to compactness is the controllability of output characteristics such as power, frequency spectrum, phase, and extracted microwave beam.

For the most natural, cylindrical geometry, the antenna-amplifier schematic is shown in Fig. 1. The annular electron beam propagates between the dielectric rod antenna and coaxial outer conductor, where it is dumped following magnetic field lines, and the RF signal enters the interaction region through the antenna feed waveguide serving simultaneously as a hollow cathode holder of the compact LIA module. Due to physical principles of LIA operation, its cath-

ode holder is at ground potential from the external side; hence, it can be connected to an extraction waveguide of an external microwave source. As a result, the antenna feed signal, at the same time, serves as the traveling wave tube (TWT) RF drive. The LIA capability of high rep-rate operation is also a feature important for practical applications.

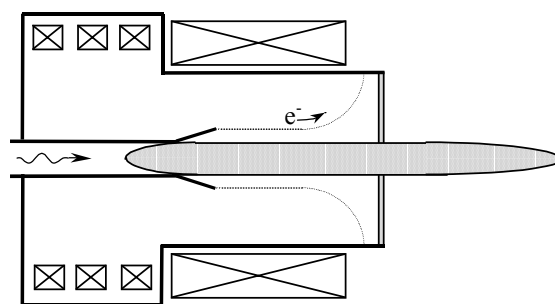


Fig. 1. Hybrid antenna-amplifier (schematic). The feed waveguide of the rod antenna is the cathode holder of LIA module. It is at ground potential. The generated electron beam amplifies the feed signal due to the TWT interaction mechanism

In this paper, the main results obtained in the course of exploration of the described concept are presented. The configuration shown in Fig. 1 represents a kind of Cherenkov maser operating in the fundamental mode of the dielectric rod antenna, the non-axisymmetric HE_{11} mode. So, theoretical studies and numerical simulations were devoted to particular issues of Cherenkov interaction between the beam and antenna slow-wave structures. Other issues are the design of the LIA module incorporating the rod antenna with its feed waveguide and experimental studies of the annular beam transport in a guiding magnetic field with the dielectric rod inside.

2. Linear Theory

The development of the linear theory of Cherenkov interaction in the general, non-axisymmetric case [1] was the first step in the exploration of the antenna-amplifier concept. The main question for the linear theory was whether the beam interaction with the HE_{11} mode is strong enough to achieve a reasonable

¹ The work was supported by the European Office of Aerospace Research and Development (EOARD) through the ISTC Partner Project No. 2823p.

gain and, in addition, to provide domination of this mode in the instability spectrum over other modes, in particular, the TM_{01} mode, which is more typical for conventional TWTs.

In Fig. 2, the calculated instability spectra are shown for two character sets of parameters. One can see that for X-band frequencies, the gain in the HE_{11} mode turns out to be about 1 dB/cm for both cases, that is quite acceptable for a relativistic TWT, but the two plots show different situations with regard to the HE_{11} mode prevalence. For the bottom plot, there is a clearly expressed domination, whereas for the top plot, growth rates in several modes are of the same order. The parameters providing domination seem more appropriate for initial proof-of-principle experiments, in spite of much narrower bandwidth making more difficult the beam voltage adjustment to obtain a gain at a given frequency of the external microwave signal.

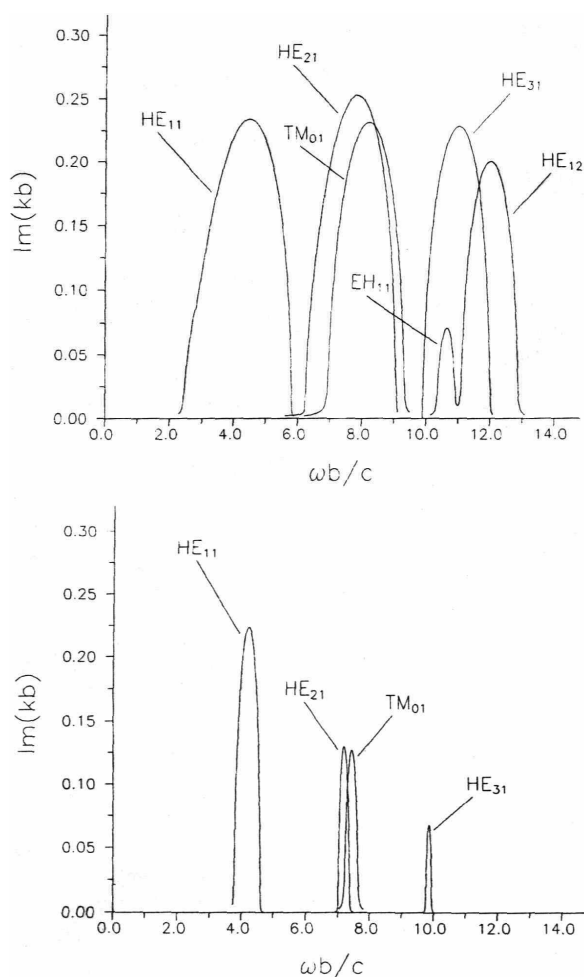


Fig. 2. Calculated growth rates in various modes for a monoenergetic, infinitely thin electron beam of current I_b , Lorenz factor γ , and radius r_b , propagating between a rod of radius a and dielectric constant ϵ and a conducting wall of radius b . At the top plot, $\epsilon = 2.25$, $a/b = 0.5$, $r_b/b = 0.6$, $I_b = 1.7$ kA, $\gamma = 1.8$. At the bottom plot, $\epsilon = 5$, $a/b = 0.3$, $r_b/b = 0.5$, $I_b = 1$ kA, $\gamma = 1.4$

Another important question for the linear theory concerns the doubts about using a dielectric. Since a dielectric structure can suffer from surface charge build-up when interacting with a beam, it is of interest to consider the case of a conducting surface wave antenna and compare achievable values of gain and bandwidth. The linear theory for the disc-loaded rod antenna has been developed [4] in the one-wave approximation, i.e., not taking the space harmonics into account. In difference of the dielectric rod case, the fundamental mode of the structure comprising a disc-loaded rod and outer circular waveguide is not the HE_{11} mode, but the quasi-TEM mode, which is axisymmetric and has no cut-off frequency. As a result, the gain-bandwidths in this mode turn out to be significantly wider than shown in Fig. 2, and spatial growth rates are much higher due to stronger beam-wave coupling at given beam-rod distances. However, for the dielectric rod, as is seen from Fig. 2, the amplification band in the fundamental HE_{11} mode is very well frequency-separated from those in higher-order modes. This is not the case with the disc-loaded rod, and this will result in difficulties with the RF drive input. In addition, the conducting rod should not be in contact with the cathode that contributes to the problem of RF input as well. For the disc-loaded rod, it is still necessary to take space harmonics into account to consider the beam interaction with the non-axisymmetric HE_{11} mode, whose amplification band is close to that of the quasi-TEM mode.

3. 1-D Nonlinear Multi-Mode Theory

As was mentioned above, for the configuration of Fig. 1, the amplification band of the lowest HE_{11} mode is well separated from other modes. Nevertheless, it is seen from Fig. 2 that multiples of the HE_{11} mode amplification band frequencies may reside within the amplification bands of the higher-order modes. That means the effect of harmonic generation due to the beam interaction with higher-order modes at the nonlinear stage can take place in the antenna-amplifier. The nonlinear theory allowing us to perform 1-D multi-mode simulations of the device was built in [5]. It is similar to the nonlinear TWT theory but takes into account an arbitrary number of modes potentially synchronous to the beam at some harmonic of the main frequency and the azimuthal asymmetry of their RF fields.

The 1-D simulations carried out for different parameters have shown that the drive signal frequency can be quite effectively multiplied. In Fig. 3, the result of the simulation accounting for five modes at three harmonics of the main frequency is presented. The parameters here correspond to the top plot of Fig. 2, with no HE_{11} mode prevalence in linear growth rate over higher-order modes. The drive signal frequency corresponds to the exact velocity synchronism of the HE_{11} mode and the beam. One can see from Fig. 3 that

the variation of the interaction region length over the range of about 20 cm leads to a dramatic change of the output signal harmonics content. Different coordinates correspond to the domination of the main frequency, to the case of comparable powers at the first, second, and third harmonics, or to the domination of the second harmonic frequency with the third harmonic middle and the main frequency lowest power. As a result, not only frequency multiplication takes place in the antenna-amplifier, but also the control of the harmonic content in the output signal spectrum is possible, so that novel tuning schemes can be realized.

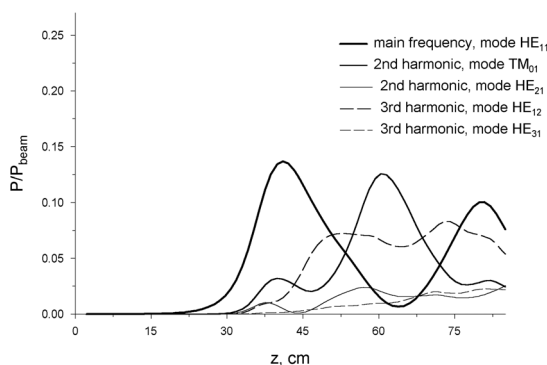


Fig. 3. Microwave powers (normalized to the beam kinetic power) of the five modes vs axial coordinate. Parameters are the same as in the top plot of Fig. 2, $b = 2$ cm. The drive signal frequency is ≈ 9.4 GHz; input power is ≈ 13 kW

At the same time, under the parameters providing the domination of the HE_{11} mode in the instability spectrum, no considerable output power at multiple frequencies is observed in the simulations. The set of parameters of the bottom plot of Fig. 2, for example, yields the second harmonic power level at least 20 dB lower than that of the main signal at 9.5–9.9 GHz range corresponding to amplification. The efficiency of the antenna-amplifier calculated in the simulations in this case exceeds 30%. Hence, these parameters can be chosen for initial experiments to prove the antenna-amplifier concept.

4. LIA Design

The design of the LIA module appropriate for an antenna-amplifier device was first discussed in [6]. At present, the module has been constructed and is being used in the model experiments on beam transport. Its scheme employs the multi-channel spark gap for switching the strip forming lines wound around the induction system to discharge them through the turns surrounding the induction cores.

There are 7 ferromagnetic toroidal cores pressed together by 12 studs between the end flanges. The studs, along with the central high-voltage electrode, form the turn, on which the electromotive forces of excitation of all the cores are added. Magnetization turns are connected to the strip electrodes of 6 parallel double forming lines. The potential electrodes are

mounted at the common arm, and the grounded electrodes are brazed to the inner surface of LIA tank. The strip width is determined by the amount and dimensions of the induction cores; the length is chosen to provide an acceptable voltage pulse duration.

The accelerating voltage produced in the LIA is applied to the cathode of the coaxial magnetically insulated diode. The diode cathode and anode diameters are 20 and 60 mm, respectively. The anode tube is further tapered to the drift tube of 40 mm diameter. The diode geometry provides ~ 1 kA beam current at 260–270 kV applied; in the drift tube, the electrons energy becomes ~ 200 keV due to space charge potential depression. Thus, the parameters corresponding to the bottom plot of Fig. 2, which were chosen for the model experiments on beam transport, are provided. The inside of high-voltage electrode is to be designed for optimal transmission of an external X-band microwave signal through a rectangular-to-circular waveguide transformer.

The LIA module is shown in Fig. 4 along with the long solenoid employed for the experiments on beam transport with the rod inside (a much shorter solenoid is planned to be used for experiments with the microwave drive signal). The dimensions of the module itself (along with the power supply) are 60 cm diameter and 100 cm length.

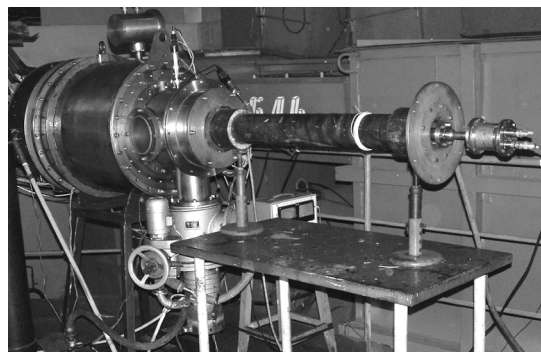


Fig. 4. Appearance of the LIA module and setup used in the model experiments on beam transport

5. 3-D Particle-in-Cell Simulations

Numerical experiments using 3-D particle-in-cell simulations represent an important component of the antenna-amplifier concept exploration. First results of the device simulations using the 3-D version of the MAGIC code have been recently obtained for an idealized geometry shown in Fig. 5 and under some simplifying conditions.

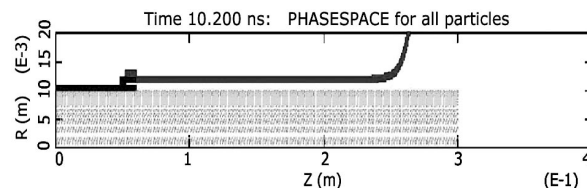


Fig. 5. System geometry and beam axial cross-section in MAGIC simulations of the antenna-amplifier

The input X-band signal was injected from the left into the inner waveguide of 1 cm radius totally filled with the dielectric ($\epsilon = 2.25$) in its fundamental TE₁₁ mode. The outer part of the left boundary (outer conductor placed at 2 cm radius) and the right boundary were set as FREESPACE. The beam was produced from the emitter of 1 mm thickness and 1.2 cm mean radius. The model of emission was set as EMISSION BEAM with 500 kV beam voltage and 1 kA current. These parameters are close to those of the top plot of Fig. 1. The beam was guided by a strong preset magnetic field (3.0 T); the dielectric rod was an extension of the input waveguide medium.

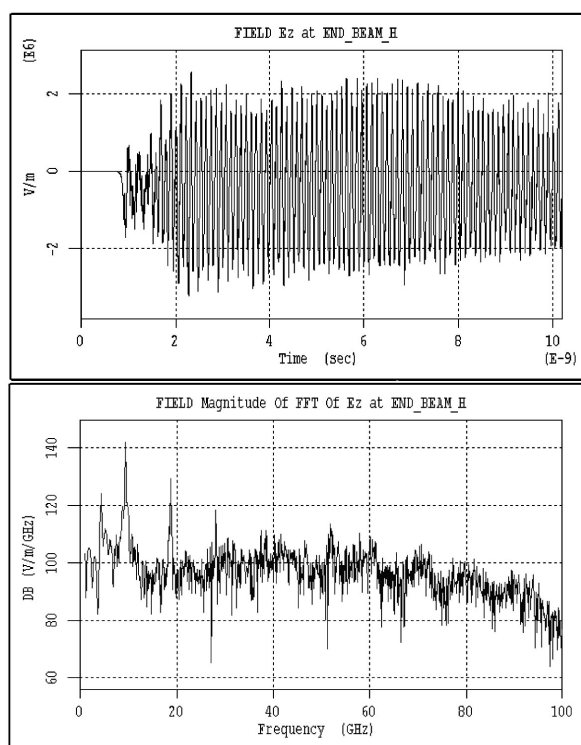


Fig. 6. Axial electric field component (top) and its spectrum (bottom) at the rod surface and $z = 24$ cm (beam end). Output microwave power is ~ 10 MW

In this model, the gain and linear amplifier response have been observed for non-axisymmetric input RF signal as well as saturation at increased interaction length. In addition, the effect of the generation of harmonics of the main frequency, found in 1-D modeling, has been verified. In Fig. 6, the axial electric field time behavior and its FFT are presented for illustration. It is seen that the frequency of the input signal (9.38 GHz, at ~ 1 MW power) is the dominant

in the spectrum. The azimuth of the point of observation here corresponds to the input wave polarization; and the spectrum looks like a noise for the azimuth at which the input wave $E_r = 0$. Some asymmetry of E_z behavior with regard to zero line at the top plot reflects the contribution of the beam space charge field. It should be noted that the absolute value of E_z field at the rod surface is ~ 20 kV/cm here that seems acceptable from the standpoint of surface breakdown.

6. Annular Beam Transport with a Dielectric Inside

The model experiments on beam transport in the absence of an external microwave signal are supposed to clarify whether plasma formation occurs at the surface of the dielectric rod. Plasma can be produced either due to placing the rod inside the cathode of the coaxial magnetically insulated diode or as a result of some beam interception during its propagation through the interaction space. It is important to measure the density of this plasma; if its order of magnitude does not exceed 10^{12} cm^{-3} (that means the plasma frequency is less than the operating frequency of the X-band), the presence of plasma does not affect the electrodynamic properties of the system, so that the concept can be realized. For the plasma density measurements, it is intended to use special collectors and Langmuir probes.

At the moment of submission the manuscript, the experiments with the dielectric rod inside have just been started. Their first results are to be reported directly at the Symposium.

References

- [1] A.S. Shlapakovski, *Tech. Phys. Lett.* **25**, 267 (1999) [*Pis'ma v ZhTF* **25**(7), 43 (1999)].
- [2] A.S. Shlapakovski, in: "*Intense Microwave Pulses VI*", *SPIE Proc.*, V. 3702, 1999, pp. 108–113.
- [3] E. Schamiloglu, in: *Conf. Record of the 25th Int. Power Modulator Symposium and 2002 High Voltage Workshop*, 2002, pp. 694–698.
- [4] A.S. Shlapakovski, in: *Proc. 13th Symp. on High-Current Electronics*, 2004 (this issue).
- [5] A.S. Shlapakovski, E. Schamiloglu, and I.I. Grushin, *Technical Physics* **47**, 1434 (2002) [*ZhTF* **72**(11), 90 (2002)].
- [6] A.S. Shlapakovski, I.I. Vintzenko, in: *Conf. Record of the 25th Int. Power Modulator Symposium and 2002 High Voltage Workshop*, 2002, pp. 510–512.